PNAS
www.pnas.org

Supplementary Information for

Enteroendocrine and tuft cells support Lgr5+ crypt stem cells upon Paneth cell ablation.

Johan H. van Es[1,2], Kay Wiebrands[1], Carmen López-Iglesias[3], Marc van de Wetering[1,2,4], Laura Zeinstra[1,2], Maaike van den Born[1,2], Jeroen Korving[1], Nobuo Sasaki[1], Peter J. Peters[3], Alexander van Oudenaarden[1,2] and Hans Clevers[1,2,4].

[1] Hubrecht Institute for Developmental Biology and Stem Cell Research-KNAW & University Medical Centre Utrecht, Utrecht, Netherlands.

[2] Oncode institute, Hubrecht Institute-KNAW, the Netherlands.

[3] The Maastricht Multimodal Molecular Imaging Institute, Maastricht University, Maastricht, the Netherlands.

[4] The Netherlands Princess Maxima Center for Pediatric Oncology, Utrecht, the Netherlands

Corresponding author: Hans Clevers
Email: h.clevers@hubrecht.eu

This PDF file includes:

Figs. S1 to S7
Table S1
References for SI reference citations

Other supplementary materials for this manuscript include the following:

Datasets S1

www.pnas.org/cgi/doi/10.1073/pnas.1801888116

Material and Methods

Generation of mice. All mouse experiments were conducted under a project license granted by the Central Committee Animal Experimentation (CCD) of the Dutch government and approved by the KNAW-Hubrecht Institute Animal Welfare Body (IvD).

pLys-^{dsRED}, pLys-^{CreErt2} or pLys-^{DTR} mice were generated through homologous recombination in IB10 embryonic stem cells (129/Ola). The DTR and CreErt2 genes were knocked onto the ATG of lysozyme, while dsRED is expressed via an IRES sequence downstream of the lysozyme gene.

The 5' primed flanking arm for the pLys-^{dsRED} contruct (3142 bp) was amplified using the following 2 primers 5'-ctcgaggatgaaaggaggtcgggagtga-3' and 5'-acgcgttcagactccgcagttccgaatata-3', while the 3' primed flanking arm (2065 bp) was amplified using the following 2 primers 5'-gcggccgcttct actgcagcccattct-3' and 5'-gcggccgccagttggttgtgagccttca-3'.

The 5' primed flanking arm for the pLys-^{DTR} and pLys-^{CreErt2} contruct (2266 bp) was amplified using the following 2 primers 5'-ctcgagagtgccctttccgtcttgtgtc-3' and 5'-acgcgtgaattcggctgggtcagc tgctggctga-3', while the 3' primed flanking arm (1686 bp) was amplified using the following 2 primers 5'-gcggccgcccaggccaaggtctacaat-3' and 5'-gcggccgccatagtcggtgcttcggtctc-3'.

The flanking arms were generated by high-fidelity PCR reactions from male 129/Ola-derived BAC DNA and subsequently cloned into vector PL451. The targeting construct (100μg) was linearized and transfected into male 129/Ola-derived IB10 embryonic stem cells by electroporation (800V, 3F). Recombinant embryonic stem cell clones expressing the neomycin gene were selected in medium supplemented with G418 (250μg/ml). Single recombinant embryonic stem cell clones were screened by Southern blotting. The frequency of homologous recombination of pLys-^{dsRED}, pLys-^{CreErt2} or pLys-^{DTR} construct was 0.25%, 4%, and 6% resp. Positive clones were selected and injected into C57BL/6 derived blastocysts using standard procedures. All injected clones gave germline transmission. The neomycin selection cassette was flanked by Frt recombination sites and excised *in vivo* by crossing the mice with the general FLP deleter strain (Jackson Lab.). Mouse tails genomic DNA were used for genotyping by PCR using allele-specific primers or dsRed, Cre or DTR specific primers.

pLys-^{dsRED}, forward: 5'-gcatgcctactggaacaggtggtggcgg-3' and
pLys-^{dsRED}, reverse: 5'-gcatgcctactggaacaggtggtggcgg-3'. Size mutant PCR band: 680bp.

pLys-^{CreErt2}, forward: 5'-cctgctttacgcacagatca and
pLys-^{CreErt2} reverse 5'-aaaggccaccccaaaatcaag-3' (lysozyme specific) and 5'-cagcccggaccgacgatg aa-3' (CreErt2 specific). Size wild type PCR band: 700bp and size mutant PCR band: 450bp.

pLys-^{DTR}, forward 5'-cctgctttacgcacagatca-3' and
pLys-^{DTR}, reverse 5'-cccatgacacctctctccat-3'. Size mutant PCR band: 561bp.

DsRed, forward: 5'-atggatagcactgagaacgt-3' and
DsRed, reverse: 5'-agcttcagcgccttgggat-3'. Size mutant PCR band: 500bp.

CreErt2, forward: 5'-ccgggctgccacgaccaa-3' and
reverse: 5'-ggcgcggcaacaccattttt-3'. Size mutant PCR band: 445bp.

DTR, forward: 5'-tgaagctgctgccgtcggtggtgctg-3' and
reverse: 5'-ctcagtgggaattagtcatgcccaact-3'. Size mutant PCR band: 550bp.

All other mice lines were described elsewhere (1-4).

Treatment of pLys-^{DTR} and pLys-^{CreErt2} mice. Adult Plys-^{DTR} and wildtype control mice (6-16 weeks) were IP injected with 0.6µl/10gr of Diphtheria-Toxin solution (1 mg/ml)(Sigma Aldrich) in PBS every 24 hours for the indicated period after which the intestines were isolated for further analysis. We analyzed at least 4 females and 4 males per time point.

The Cre enzyme, present in the pLys-^{CreErt2} KI mice, was induced by a single intraperitoneal injection of Tamoxifen (5mg in 200µl/25gr)(Sigma Aldrich) dissolved in sunflower oil. The 6-16 weeks old pLys-^{CreErt2} mice, as well as various genotypic controls, were sacrificed and the complete intestines were isolated for further analysis. We analyzed the intestines derived from 10 (4 females and 6 males) tamoxifen-induced pLys-^{CreErt2}_Rosa^{LSL}-^{LacZ} mice and 4 uninduced pLys-^{CreErt2}_Rosa^{LSL}-^{LacZ} mice.

Immunohistochemistry. Experiments were performed as described before (5). Freshly isolated intestines were flushed with formalin (4% formaldehyde in PBS) and fixed by incubation in a tenfold excess of formalin overnight at room temperature. The formalin was removed and the intestines washed twice in PBS at room temperature. The intestines were then transferred to a tissue cassette and dehydrated by serial immersion in 20-fold volumes of 70%, 96% and 100% EtOH for 2 hours each at 4°C. Excess ethanol was removed by incubation in xylene for 1.5 hours at room temperature and the cassettes then immersed in liquid paraffin (56°C) overnight. Paraffin blocks were prepared using standard methods.

4µm tissue sections were de-waxed by immersion in xylene (2 times 5min) and hydrated by serial immersion in 100% EtOH (2 times 1min), 96% EtOH (2 times 1min), 70% EtOH (2 times 1min) and distilled water (2 times 1min). Endogenous peroxidase activity was blocked by immersing the slides in peroxidase blocking buffer (0.040 M citric acid, 0.121M disodium hydrogen phosphate, 0.030M sodium azide, 1.5% hydrogen peroxide) for 15min at room temperature. Antigen retrieval was performed (see details below for each antibody), and blocking buffer (1% BSA in PBS) added to the slides for 30min at room temperature. Primary antibodies were then added and incubated as detailed below. The slides were then rinsed in PBS and secondary antibody added (polymer HRP-labeled anti-mouse/rabbit, Envision) for 30min at room temperature. Slides were again washed in PBS and bound peroxidase detected by adding DAB substrate for 10min at RT. Slides were then washed 2 times in PBS and nuclei counterstained with Mayer's hematoxylin for 2min, followed by two rinses in distilled water. Sections were dehydrated by serial immersion for 1 min each in 50% EtOH and 60% EtOH, followed by 2min each in 70% EtOH, 96% EtOH, 100% EtOH and xylene. Slides were mounted in Pertex mounting medium and a cover slip placed over the tissue section. Antigen retrieval was performed by boiling samples for 20min in 10mM sodium citrate buffer pH 6.0. Antibodies used were; rabbit anti-synaptophysin (1:200 dilution); Dako rabbit anti-lysozyme (1:1750 dilution; DAKO), rabbit anti-Dcamkl1 (1:200 dilution; Abcam), mouse anti-BrdU (1:100 dilution; Dako) and Rabbit anti-Olfm4 (1:200 dilution; Cell Signaling). Incubation of antibodies was performed O/N in BSA in PBS at 4°C for the antibody directed against BrdU, Dcamkl1 and Olfm4 and for 1hr at room temperature for antibodies directed against synaptophysin, and lysozyme. In all cases, the Envision^{+} kit (Dako) was used as a secondary reagent. Stainings were developed with DAB. Slides were counterstained with hematoxylin and mounted.

***in situ* hybridization** For *in situ* hybridization, 8µm-thick sections were rehydrated as described above. Afterwards, the sections were treated with 0.2M sodium chloride and proteinase K. Slides were postfixed, and sections were then demethylated with acetic anhydride and prehybridized.

Hybridization was done in a humid chamber with 500ng/ml freshly prepared digoxigenin (DIG)-labeled RNA probe of Olfm4 (image clone 1078130) or cryptdin-1 (image clone 1096215). Sections were incubated for at least 48hrs at 68°C. The slides were washed and incubation of the secondary anti-DIG antibody (Roche) was done at 4°C overnight. The next day, sections were washed and developed using Nitro Blue Tetrazolium Chloride/5-Brom-4-Chlor-3-Indolyl-Phosphate.

Single-molecule fluorescent *in situ* hybridization. As described previously (6), the duodenum/jejunum was quickly dissected, flushed with cold 4% paraformaldehyde in PBS, and incubate at 4^0C for 2-3hrs with gentle agitation. Subsequently, the tissue was put into a pre-chilled cryoprotecting solution (4% paraformaldehyde/30% sucrose/PBS) and incubated overnight at 4^0C with gentle agitation. After the O/N incubation, the tissue was put into the molds filled with cold OCT and stored at -80^0C. Probe libraries were designed and constructed as described. Hybridizations were done overnight with differentially labeled probes using Cy5 (Hes1, synaptophysin) and TMR (Lgr5) fluorophores. An additional FITC conjugated antibody for E-Cadherin (BD Biosciences) was added to the hybridization mix and used for protein immunofluorescence to detect cell borders. DAPI dye for nuclear staining was added during the washes. Images were taken with a Perkin Elmer Ultraview Spinning disk. All images are filtered with a Laplacian of Gaussian filter and are maximal projections of 15 stacks spaced 0.3μm apart in the Z direction.

X-gal staining. As described previously (5). To determine the pattern of Cre-mediated recombination of the $Rosa^{LSL\text{-}LacZ}$ reporter locus on day 10 upon Tamoxifen induced Cre induction, the complete intestines derived from 14 pLys-^{CreErt2}_$Rosa^{LSL}$-^{LacZ} mice (10 Tamoxifen induced and 4 uninduced)(age 6-16 wks) were isolated and immediately flushed with ice-cold fixative (1 % formaldehyde, 0.2 % glutaraldehyde, 0.02 % NP40 in PBS0 (phosphate-buffered saline deficient in Mg^{2+} and Ca^{2+})) and incubated for 2 hours in a 20-fold volume of the same ice-cold fixative at 4°C on a rolling platform. The fixative was removed and the intestines washed twice in PBS0 for 20 min. at room temperature on a rolling platform. The β-galactosidase substrate (5 mM $K_3FE(CN)_6$, 5 mM $K_4Fe(CN)_6 \cdot 3H_20$, 2 mM $MgCl_2$, 0.02% NP40, 0.1 % Nadeoxycholate, 1 mg/ml^{-1} X-gal in PBS0) was then added and the tissues incubated in the dark overnight at room temperature. The substrate was removed and the tissues washed twice in PBS0 for 20 min. at room temperature on a rolling platform. The tissues were then fixed overnight in a 20-fold volume of 4% paraformaldehyde (PFA) in PBS0 at 4°C in the dark on a rolling platform. The PFA was removed and the tissues washed twice in PBS0 for 20 min. at room temperature on a rolling platform. The stained tissues were transferred to tissue cassettes and paraffin blocks prepared using standard methods. Tissue sections (4 μM) were prepared and counterstained with neutral red

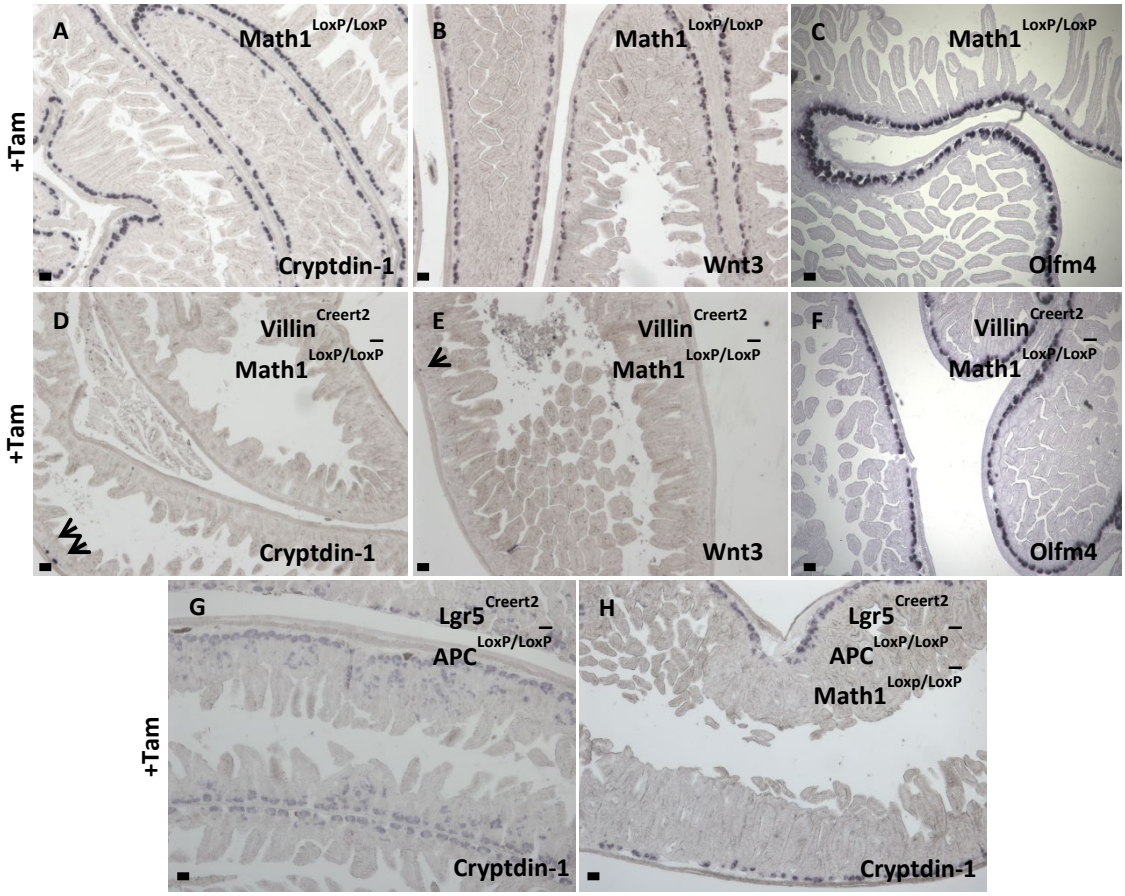

Fig. S1. Presence of functional Lgr5^{+} intestinal stem cells and the formation of APC tumors in the complete absence of Paneth cells upon epithelial Math1 deletion. *In situ* hybridization analysis of the intestine derived from Math1$^{LoxP/LoxP}$_Villin^{CreErt2} mice (*D*, *E*, *F*) and control Math1$^{LoxP/LoxP}$ mice (*A*, *B*, *C*) upon tamoxifen-induced Cre expression. The absence of Math1 resulted in the absence of cryptdin-1^{+} (*D* versus *A*) and Wnt3^{+} (*E* versus *B*) Paneth cells, while the Olfm4^{+} intestinal stem cells were not affected (*F* versus *C*). Black arrows in *D* and *E* indicate the presence of single cryptdin-1^{+} and Wnt3^{+} Paneth cells in the intestine of DT treated mice, resp. The formation of intestinal APC tumors from the Lgr5^{+} stem cell is either affected by the absence of cryptdin-1^{+} Paneth cells (*H* versus *G*). Scale bar = 100 µm.

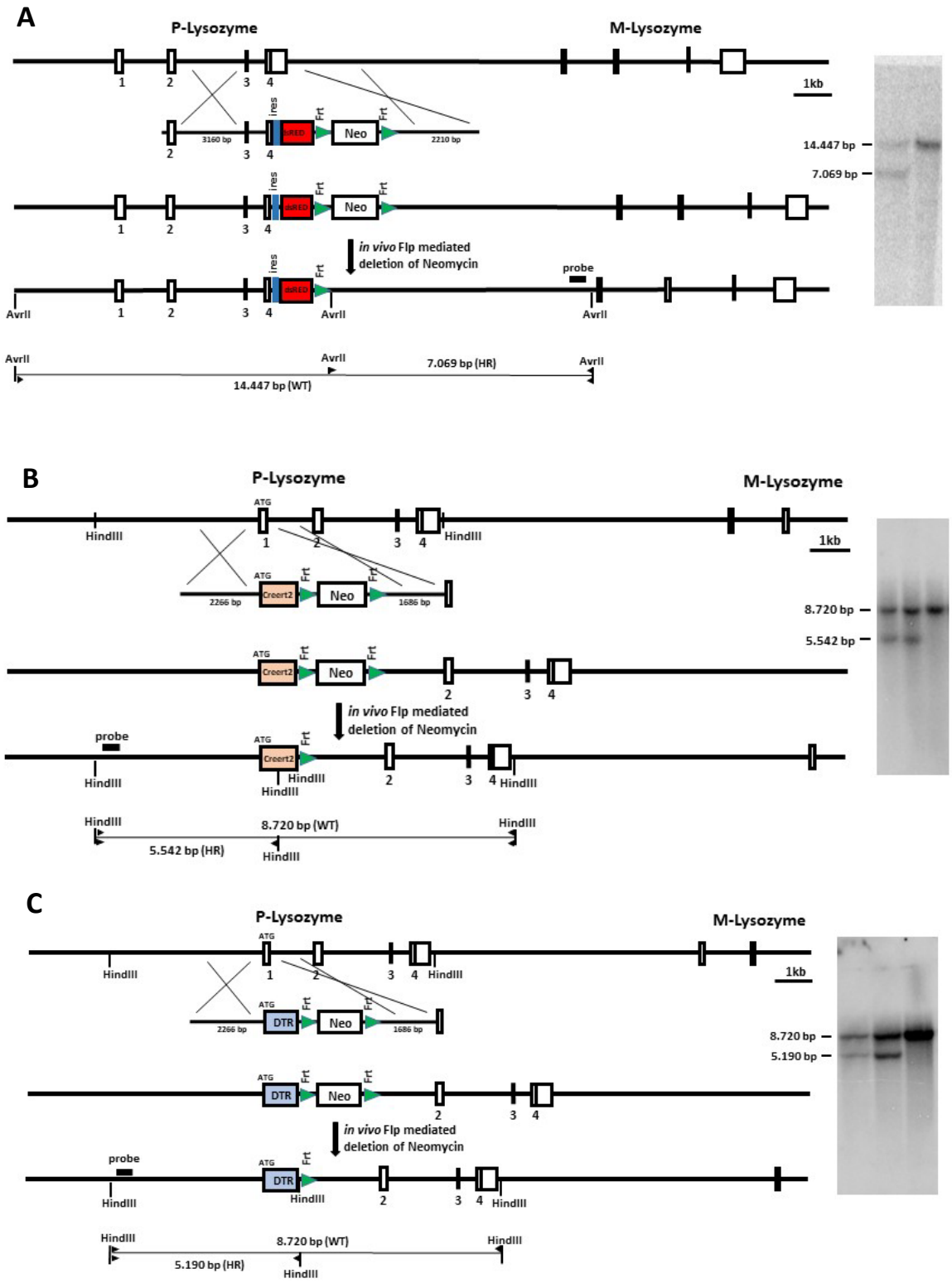

Fig. S2. The targeting constructs used to generate the pLys-^{dsRED}, pLys-^{CreErt2} and pLys-^{DTR} KI mice.

The diagrams showed the targeting constructs, the wild type, and the targeted locus **before and after** Flp or Cre mediated recombination. Southern blot analysis showed successful homologous recombination.

(*A*) pLys-^{dsRED} mice. From top to bottom. The gene structure of the P-Lys allele and the pLys-^{dsRED} construct. Homologous recombination of the pLys-^{dsRED} construc**t** into the P-Lys locus resulted in the insertion of the Neomycin resistance gene cassette, surrounded by FLP sites, and the IRES-dsRED gene just after the stop codon of Exon 4. The thick black line indicates the probe used for genomic Southern-blot analysis. DNA isolated from transfected and control ES cells was digested with the AvrII restriction enzyme. The 14.447 Kb band corresponds to the wild-type allele and the 7.069 Kb band correspond to the correct integration of the targeting construct. 0.25% of the neomycin selected ES cells had undergone homologous recombination. The Neomycin gene was deleted *in vivo* via FLP recombination in the FLP deletor strain.

(*B*) pLys-^{CreErt2}. From top to bottom. The gene structure of the P-Lys allele and the pLys-^{CreErt2} construct. Homologous recombination of the pLys-^{CreErt2} construct into the P-Lys locus resulted in the insertion of the Neomycin resistance gene cassette, surrounded by FLP sites, and the CreErt2 gene on the ATG start codon of the exon 1 of the pLys gene. The thick black line indicates the probe used for genomic Southern-blot analysis. DNA isolated from transfected and control ES cells was digested with the HindIII restriction enzyme. The 8.720 Kb band corresponds to the wild-type allele and the 5.542 Kb band corresponds to the correct integration of the targeting construct. 4% of the neomycin selected ES cells had undergone homologous recombination. We generated pLys-^{CreErt2} KI mice from 2 independent ES cell clones. The Neomycin gene was deleted *in vivo* via FLP recombination in the FLP deletor strain. The analysis of both lines revealed that they gave the same phenotype. All described experiments were subsequently performed with 1 line.

(*C*) pLys-^{DTR} mice. From top to bottom. The gene structure of the P-Lys allele and the pLys-^{DTR} construct. Homologous recombination of the pLys-^{DTR} construc**t** into the P-Lys locus resulted in the insertion of the Neomycin resistance gene cassette, surrounded by FLP sites, and the DTR gene on the ATG start codon of the exon 1 of the pLys gene. The thick black line indicates the probe used for genomic Southern-blot analysis. DNA isolated from transfected and control ES cells was digested with the HindIII restriction enzyme. The 8.720 Kb band corresponds to the wild-type allele and the 5.190 Kb band correspond to the correct integration of the targeting construct. 6% of the neomycin selected ES cells had undergone homologous recombination. We generated pLys-^{DTR} KI mice from 2 independent ES cell clones. The Neomycin gene was deleted *in vivo* via FLP recombination in the FLP deletor strain. The analysis of both lines revealed that they gave the same phenotype. All described experiments were subsequently performed with one mouse line.

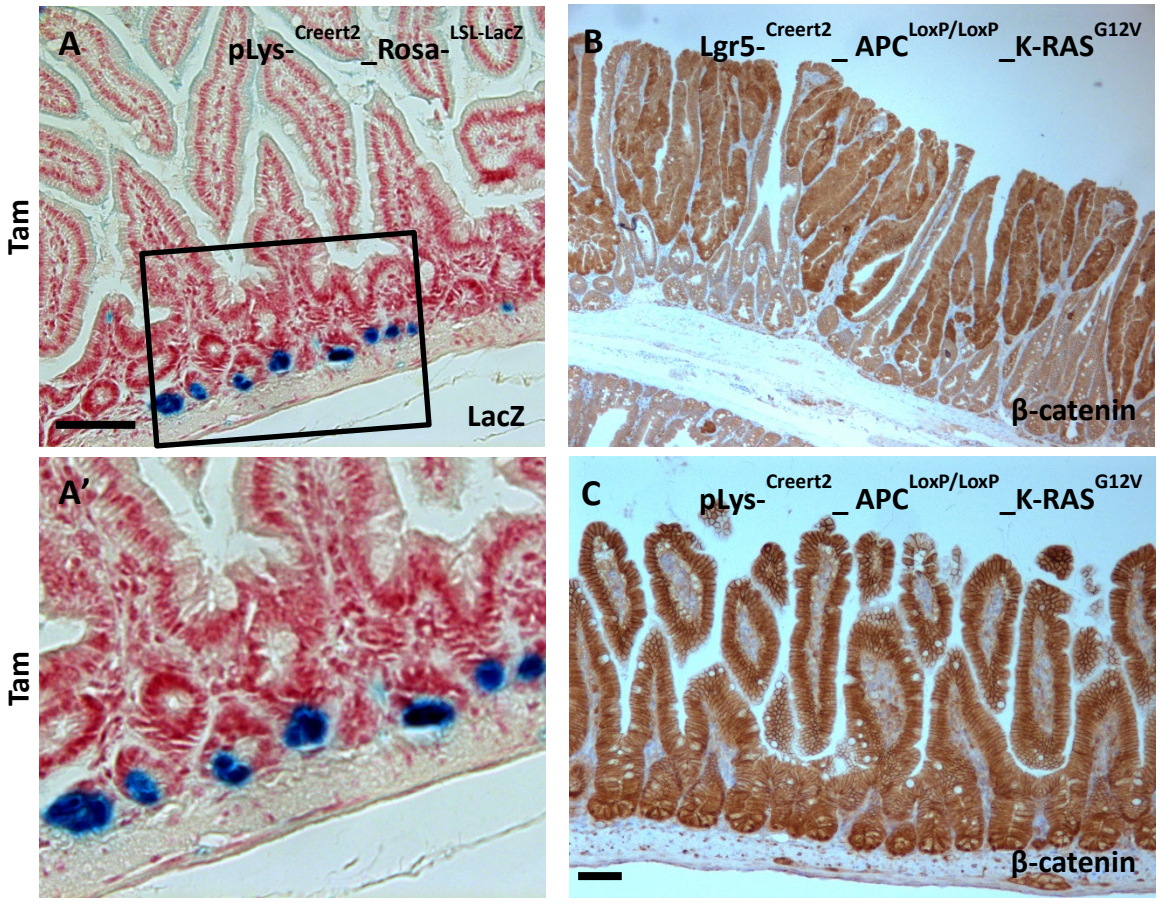

Fig. S3. Usage of pLys^{CreErt2} mice in Paneth cell-specific recombination. Histological analysis of LacZ expression in the intestine derived from pLys-^{CreErt2}_Rosa$^{LSL\text{-}LacZ}$ mice at 10 days (*A* and *A'*) post tamoxifen mediated Cre-induction revealed up to 12% of the Paneth cells expressed the LacZ reporter.

Somatic defects in *K-ras* collaborate with *APC* inactivation to promote the progression of adenomatous lesions to human colorectal cancer. K-ras mutation occurs in 40–50% of human colorectal adenomas and carcinomas. Mutation of the K-ras gene at codon 12 (glycine to valine substitution) is the most aggressive mutation associated with poor prognosis. Induced deletion of APC in the murine Lgr5+ stem cells, in contrast to the short-lived TA cells, leads to tumor formation. In addition, we have shown that Lgr5 stem cell-specific expression of oncogenic K-ras alone does not induce intestinal tumour formation. Combining apc deletion with oncogenic K-ras activation in intestinal stem cells leads to a modest increase in intestinal tumour initiation and a dramatic increase in tumour expansion We next asked our self the question whether the Paneth cells, intermingled with the Lgr5 stem cells at the bottom of the crypt, can generate tumours as well upon APC inactivation and K-ras activation.

We therefore generated the Lgr5$^{GFP\text{-}ires\text{-}CreErt2}$_APC-$^{LoxP/LoxP}$_K-ras-$^{LSL\text{-}G12D}$ and pLys^{CreErt2}_APC-$^{LoxP/LoxP}$_K-ras-$^{LSL\text{-}G12D}$ compound mice. The Lgr5$^{GFP\text{-}ires\text{-}CreErt2}$ KI mice express the tamoxifen-inducible Cre enzyme specifically in the intestinal stem cells. The K-ras^{G12D} requires the Cre-mediated elimination of a transcriptional roadblock to allow the controlled expression of

endogenous, single copy oncogenic K-ras. Cre-mediated recombination of the floxed apc allele induces the deletion of exon 14, leading to a frame-shift, which truncates and inactivates the protein after amino acid 580 and hereby activating the Wnt pathway. In the *Lgr5*$^{\text{GFP-IRES-CreErt2}}$_*Apc*$^{\text{LoxP/LoxP}}$_K-ras-$^{\text{LSL-G12D}}$ mice (n=6) and the pLys$^{\text{CreErt2}}$_Apc$^{\text{LoxP/LoxP}}$_K-ras-$^{\text{LSL-G12D}}$ mice (n=6), the Cre enzyme was activated with a single intraperitoneal injection of tamoxifen (5 mg). We had to euthanize the *Lgr5*$^{\text{GFP-IRES-CreErt2}}$_*Apc*$^{\text{LoxP/LoxP}}$_K-ras-$^{\text{LSL-G12D}}$ mice on day 10 post-Tamoxifen administration since beyond 10 days the induced genetic alterations would result in discomfort. Histological analysis of the small intestine and colon revealed the formation of many intestinal tumors (*B*). The small intestine of the pLys-$^{\text{CreErt2}}$_Apc$^{\text{LoxP/LoxP}}$_K-ras-$^{\text{LSL-G12D}}$ was isolated on day 35 post tamoxifen administration. Extensive histological analysis demonstrated the complete absence of intestinal tumor formation when APC and K-ras were specifically deleted c.q. activated in Paneth cells (*C*). Scale bar = 100 μm.

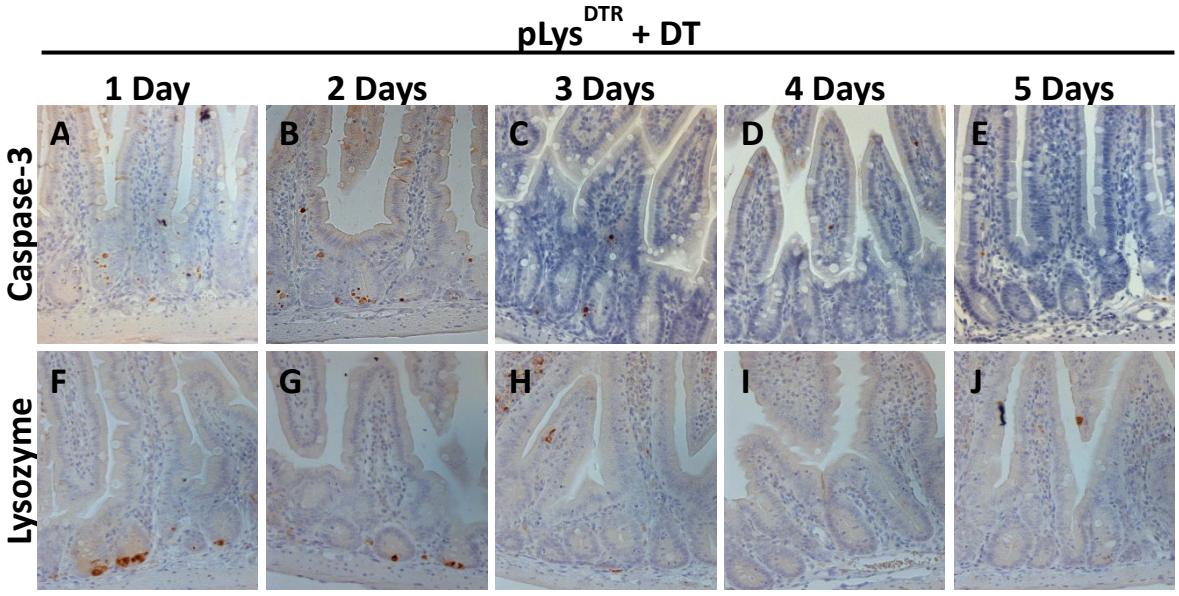

Fig. S4. Overtime deletion of Paneth cells in the pLys–^{DTR} KI mice upon DT administration. Caspase 3 (*A-E*), lysozyme (*F-J*) in the jejunum derived from the DT treated pLys–^{DTR} KI mouse at the indicated time upon daily DT injection. Scale bar = 100 μm.

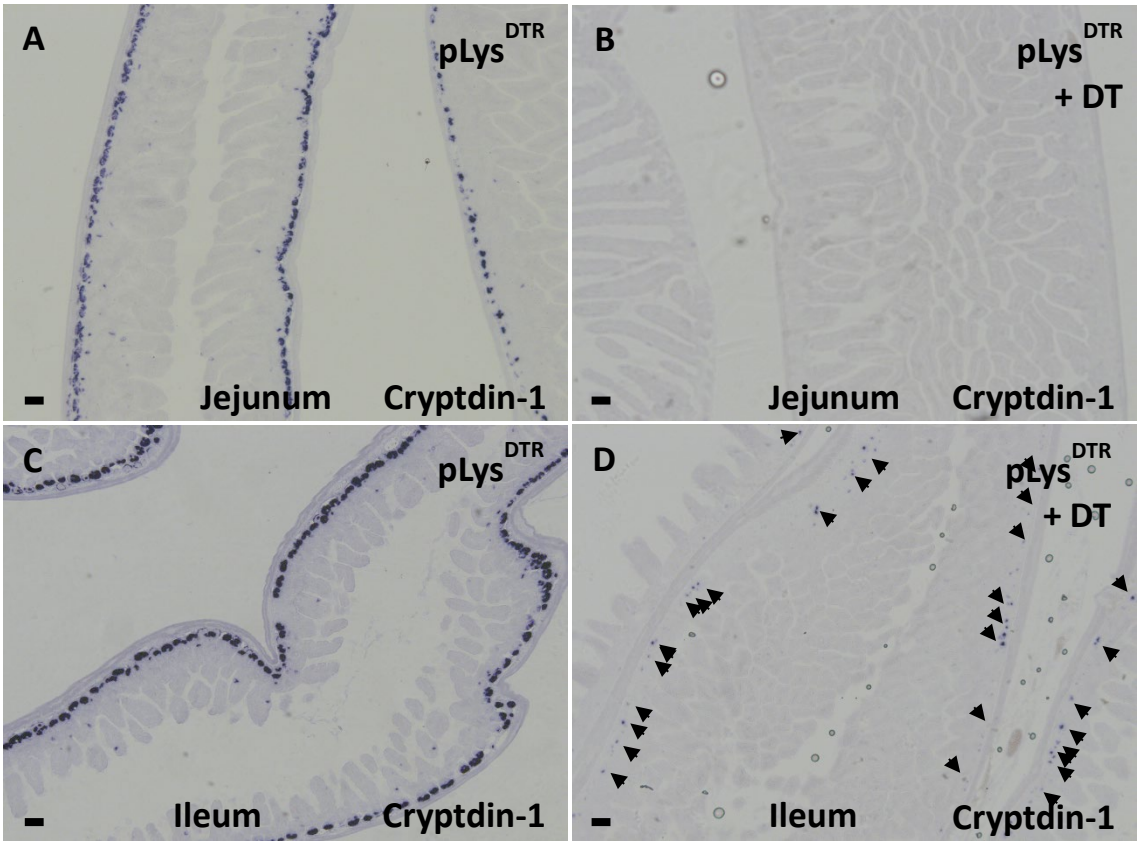

Fig. S5. Deletion of Paneth cells in different regions of the intestine in the pLys–^{DTR} KI mice upon DT administration. *In situ* hybridization of cryptdin-1 in the jejunum and ileum derived from the untreated pLys–^{DTR} KI control mice (*A*, *C*) and for 6 days DT treated pLys–^{DTR} KI mouse (*B*, *D*), 16 hrs after the last DT injection. The analysis showed the efficient deletion of Paneth cells in the Jejunum upon DT treatment, while in the ileum individual Paneth cells could still be detected. Scale bar = 100 µm. Dashed bar: max. position of BrdU positive cells.

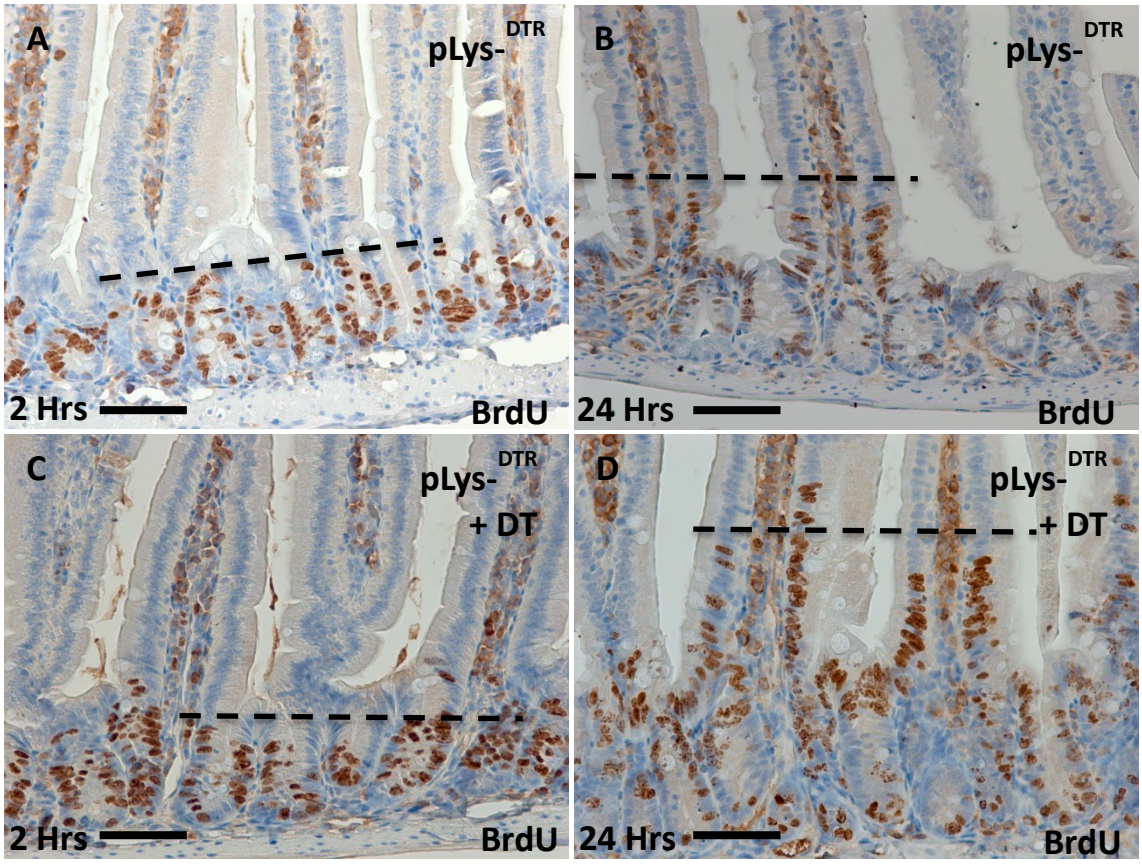

Fig. S6. Paneth cell ablation doesn't affect the proliferation of intestinal (stem) cells. Histological analysis 2 hrs (*A*, *C*) or 24 hrs (*B*, *D*) post-BrdU injection of DT treated (4 consecutive days) pLys-^{DTR} (*C*, *D*) and untreated pLys-^{DTR} control mice (*A*, *B*) showed comparable proliferation of intestinal (stem) cells via an antibody directed against BrdU. Scale bar = 100 μm.

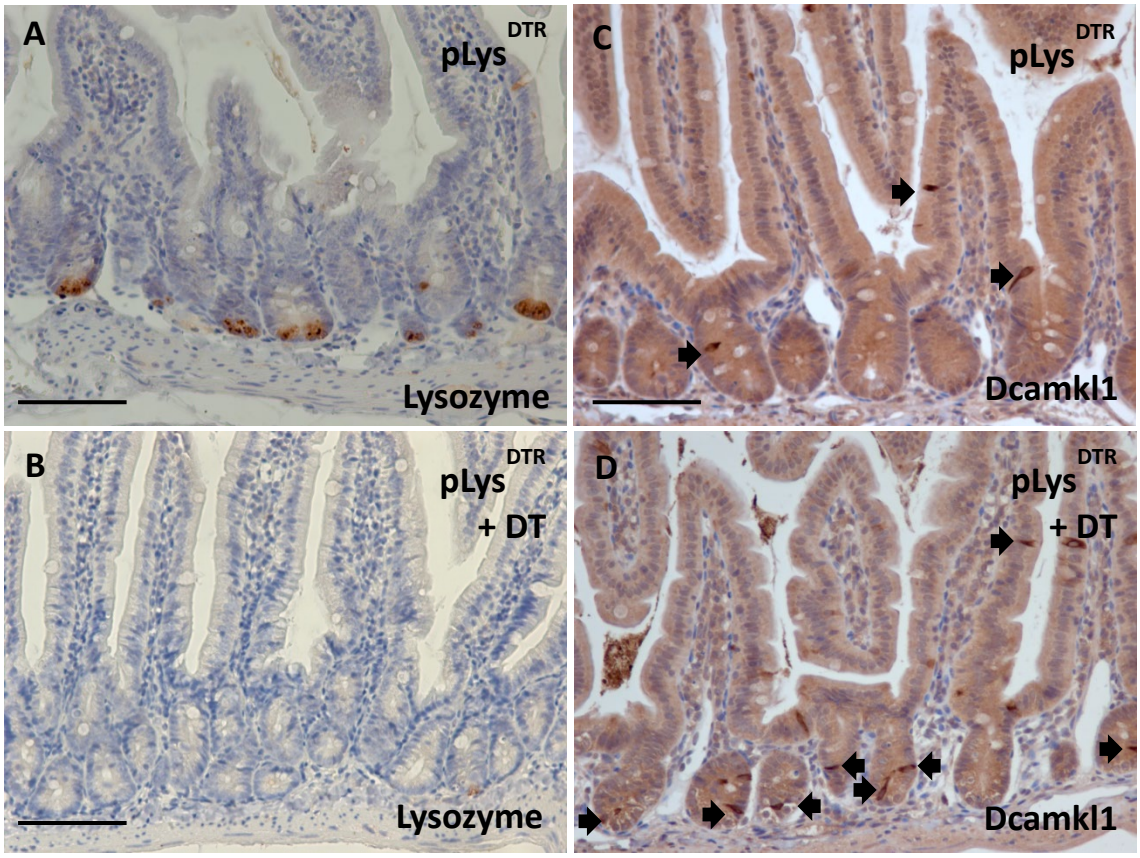

Fig. S7. Dcamkl1+ Tuft cells support Lgr5^{+} crypt stem cells upon Paneth cell ablation. Histological analysis with antibodies directed against Lysozyme (*A*, *B*) or Dcamkl1 (*C*, *D*) on sections of the intestine derived from DT-treated (for 6 days) pLys-^{DTR} KI mice (*B*, *D*) and untreated pLys-^{DTR} KI mice (*A*, *B*). This analysis revealed the presence of Lysozyme^{+} Paneth cells at the bottom of the crypt and Dcamkl1^{+} Tuft cells in the transit-amplifying zone of the crypt and on the villi (*A* and *C*, resp.) in the control mice, while in the DT-treated pLys-^{DTR} KI mice, the Paneth cells were successfully ablated and the Dcamkll1^{+} Tuft cells were intermingled with the intestinal stem cells at the bottom of the crypt (see arrows in *D*). Quantification revealed the presence of on average 0.09 Tuft cell per crypt in a single plane section (counted: 600 crypts per mouse, n=3). Scale bar = 100 μm.

	cluster 1	cluster 2	cluster 4	cluster 8	cluster 12	cluster 3	cluster 6	cluster 7	cluster 5	cluster 9	cluster 10	cluster 11	cluster 15	cluster 13	cluster 14	cluster 16
	average	average	average	average	average	average	average	average	average	average	average	average	average	average	average	average
	n=25	n=7	n=7	n=24	n=5	n=16	n=17	n=8	n=25	n=18	n=11	n=15	n=3	n=1	n=3	n=1
after DT total 116:	24	7	7	21	5	11	12	4	13	7	4	0	0	0	1	0
control total 72:	1	0	0	3	1	5	5	4	12	11	8	15	3	1	2	1
Stem cells																
Lgr4__chr2	0,26			0,23	0,30	0,35	0,39	0,23	0,14	0,27		0,30	0,43		0,43	0,32
Lgr5__chr10	0,14			0,35					0,14	0,21						
Tnfrsf19__chr14																
Smoc2__chr17	0,34	0,39		0,89	0,36	0,79	0,45	0,23	0,30	0,47	0,35	0,37		1,10	1,10	•0,77
Paneth cells																
Def6__chr17																
Def8__chr8		0,24	0,39	0,14	0,30	0,23		0,35	0,30		0,35					
Defa-rs1__chr8	10,02	0,53	0,24	0,64	0,70	1,23	3,63	0,73	0,94	12,87	1,85	60,21	5,10	1,10	1,10	1,10
Defa-rs7__chr8	0,74						0,16			0,60		2,83			0,43	
Defa17__chr8	27,89	0,81	0,67	1,06	1,10	1,16	6,15	1,48	1,26	35,25	1,35	59,95	6,10	1,10	2,10	3,60
Defa20__chr8				0,18			0,28	0,35	0,18	7,09	0,18	10,90	0,77			
Defa21__chr8	0,14	0,39		0,18		0,23		0,23	0,26	0,54		10,96	0,77			
Defa22__chr8	0,38									1,10		4,10	0,77			
Defa23__chr8	0,50						0,16			0,54		2,43	0,43			
Defa25__chr8	0,14															
Defa26__chr8	1,18			0,14		0,16	0,22		0,14	2,88	0,18	14,15				0,60
Defa3__chr8	1,70		0,24	0,18		0,16	0,34		0,22	2,93	0,43	14,49	0,43		0,43	0,60
Defa4__chr8	0,18									0,27		0,23				
Defa5__chr8	2,10	0,24		0,18		0,29	0,39	0,60	0,46	9,16	0,52	46,48	5,77			
Defa6__chr8	2,06			0,18			0,75		0,22	1,99	0,27	4,43	0,43		0,43	
Defb1__chr8	0,14											0,17				
Defb20__chr2																
Defb23__chr2																
Lyz1__chr10	18,18	3,24	1,67	1,64	3,30	2,54	14,75	2,60	4,34	130,32	3,52	185,03	25,40	3,10	4,10	18,10
Spink4__chr4	133,06	7,67	5,80	6,88	7,08	4,53	115,62	3,23	4,54	158,09	4,43	62,23	15,77	1,10	5,10	143,10
Mmp7__chr9	9,00	0,81	0,24	0,35	0,50	0,79	7,27	0,35	0,66	11,81	0,35	13,56	2,77		0,43	6,60
Muc13__chr16	2,70	3,24	0,96	1,73	1,30	1,04	3,22	1,73	1,22	2,60	2,02	3,37	3,10	4,10	3,10	6,60
Muc2__chr7	14,02	0,81	0,67	1,23	1,90	0,85	15,90	0,98	0,74	16,65	0,43	4,96	3,43		2,10	39,60
Reg4__chr3	19,80	0,67	2,10	1,85	3,70	5,23	12,56	1,73	1,06	25,04	0,93	8,97	3,77		0,77	12,10
Tuft cells																
Dclk1__chr3	0,18		0,24	3,77			0,16		0,26				1,43			
Gfi1b__chr2				0,43												
Trmp5				3.37												
Sox9	2,18	1,10	0,24	2,23	0,30	0,29	0,92		0,46	1,27		0,63	1,77			
Spib__chr7	0,18	0,39		3,10					0,30				1,77		0,43	
Goblet cells																
Spdef__chr17	2,26	0,39		0,43		0,48	1,69		0,18	1,21		0,77				1,60
Klf4__chr4	1,42	0,24	0,39	0,77	0,30	0,60	1,34	0,35	0,54	0,99	0,27	0,23	0,43			0,60
Muc13__chr16	2,70	3,24	0,96	1,73	1,30	1,04	3,22	1,73	1,22	2,60	2,02	3,37	3,10	4,10	3,10	6,60
Muc2__chr7	14,02	0,81	0,67	1,23	1,90	0,85	15,90	0,98	0,74	16,65	0,43	4,96	3,43		2,10	39,60
Enterocyte																
Fabp1__chr6				0,77							1,02			1,10	0,43	
Entero-endocrine cells																
Cck__chr9	0,38	0,53	13,81	0,56	1,30	0,79	0,45	104,23	0,86	0,16	14,01	0,30	18,77	2,10	1,73	1,10
Chgb__chr2	2,42	7,10	21,53	1,48	3,30	78,63	2,16	9,95	1,42	0,88	26,25	0,57	8,10	18,10	16,70	0,60
Sct__chr7	1,58	1,10	8,96	0,48	2,30	3,28	1,39	9,73	0,94	0,99	12,35	0,43	1,43	2,10	9,10	1,10
Ghrl__chr6	2,90	32,80	23,81	1,77	258,50	2,29	1,21	22,48	9,90	0,93	0,93	0,23	43,07			
Gcg__chr2	0,30		0,53	0,35	0,90	0,35	0,22	130,10	0,18	0,32	1,18	0,30	18,10			0,60
Sst__chr16	0,86	258,94	0,67	0,93	0,30	1,41	1,04	0,35	0,50	0,32	0,35		0,43	22,10	4,43	
Gip__chr11	1,14	7,24	3,67	1,56	0,50	1,23	2,51	1,98	1,54	1,54	271,83	2,10	14,77	3,10	73,77	1,60
Neurog3__chr10	0,38		0,24	0,14		3,35	0,16		4,06				0,43			
Reg4__chr3	19,80	0,67	2,10	1,85	3,70	5,23	12,56	1,73	1,06	25,04	0,93	8,97	3,77		0,77	12,10

Table S1. Selected gene expression of the 16 independent clusters.

Average of gene expression per cluster for intestinal epithelial-specific cell populations for selected genes.

Additional data table S1

Data set S1. Gene expression. Gene expression of 188 randomly selected, FACS sorted single cells derived from gate **a** of the DT treated pLys-^{DTR} (Fig. 5, DT; n= 116) and from gate **a** of the untreated control mice (Fig. 5C; n=72) revealed the presence of 16 independent clusters.

References

1. Barker N, *et al.* (2007) Identification of stem cells in small intestine and colon by marker gene Lgr5. *Nature* 449(7165):1003-1007.
2. van Es JH, *et al.* (2012) Dll1+ secretory progenitor cells revert to stem cells upon crypt damage. *Nat Cell Biol* 14(10):1099-1104.
3. Snippert HJ, *et al.* (2009) Prominin-1/CD133 marks stem cells and early progenitors in mouse small intestine. *Gastroenterology* 136(7):2187-2194 e2181.
4. Schepers AG, *et al.* (2012) Lineage tracing reveals Lgr5+ stem cell activity in mouse intestinal adenomas. *Science* 337(6095):730-735.
5. van Es JH, *et al.* (2012) A critical role for the Wnt effector Tcf4 in adult intestinal homeostatic self-renewal. *Mol Cell Biol* 32(10):1918-1927.
6. Itzkovitz S, *et al.* (2011) Single-molecule transcript counting of stem-cell markers in the mouse intestine. *Nat Cell Biol* 14(1):106-114.